SPACE DETECTION OF GRAVITATIONAL WAVES (LISA)

J.C. NEVES de ARAUJO[1], S. BUCHMAN[2], A. CAVALLERI[3], K. DANZMANN[4], R. DOLESI[5], G. FONTANA[5], J. HANSON[2], M. HUELLER[5], S. SIGURDSSON[6], J. TURNEAURE[2], C. UNGARELLI[7], A. VECCHIO[8], S. VITALE[5], W. WEBER[9]

Abstract

The Laser Interferometer Space Antenna (LISA) mission is designed to observe gravitational waves from galactic and extra-galactic binary systems, including gravitational waves generated in the vicinity of the very massive black holes found in the centers of many galaxies. Acting as a giant Michelson interferometer the three spacecraft flying 5 million km apart will open the era of astronomy in the gravitational spectrum. We give an introduction to the mission and describe the status of selected experimental, theoretical, and planning LISA work, as reported at the Ninth Marcel Grossman Meeting in 2000 in Rome. We discuss the three areas of technology challenges facing the mission inertial sensors, micronewton thrusters, and picometer interferometry. We report on the progress in the development of free falling moving test-masses for LISA and for the related technology demonstration mission. We present simple formulas to evaluate the performance of the device as a function of the various design parameters, and we compare them with preliminary experimental results from a test prototype we are developing. Quantitative agreement is found. The gravitational radiation emitted during the final stages of coalescence of stellar mass compact objects with low massive black holes is a signal detectable by LISA. It will also provide the opportunity of measuring relativistic strong field effects. A brief discussion addresses the detection by LISA of gravitational waves generated by cataclysmic binary variables at frequencies below 1 mHz. Finally the prospects for cosmology work with LISA type antennas are being analyzed.

1 The LISA Mission

The LISA mission[1-20] comprises three identical spacecraft located 5 x 10^6 km apart forming an equilateral triangle. LISA is basically a giant Michelson interferometer placed in space, with a third arm added to give independent information on the two gravitational wave polarizations, and for redundancy. The distance between the spacecraft —the

[1] Instituto Nacional de Pesquisas Espaciais, Sao Jose dos Campos, Brazil
[2] W.W. Hansen Experimental Physics Laboratory, Stanford University, USA
[3] CEFSA-ITC, Italy
[4] Institut für Atom- und Molekülphysik, Universität Hannover, Germany
[5] Dipartmento di Fisica, Universita di Trento and INFN, Italy
[6] Department of Astro and Astrophys, Pennsylvania State University, State College, USA
[7] School of Computer Science and Mathematics, University of Portsmouth, UK
[8] Max Planck Institut fur Gravitationphysik, Alber Einstein-Institut, Germany
[9] Consorzio Criospazio Richerche, Italy

interferometer arm length — determines the frequency range in which LISA can make observations; it was carefully chosen to allow for the observation of most of the interesting sources of gravitational radiation. The center of the triangular formation is in the ecliptic plane, 1AU from the Sun and 20° behind the Earth. The plane of the triangle is inclined at 60° with respect to the ecliptic. These particular heliocentric orbits for the three spacecraft were chosen such that the triangular formation is maintained throughout the year with the triangle appearing to rotate about the center of the formation once per year.

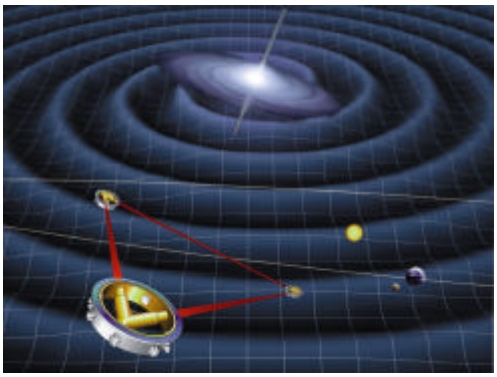

Figure 1: LISA Interferometer Geometry

While LISA can be described as a big Michelson interferometer, the actual implementation in space is very different from a laser interferometer on the ground and is much more reminiscent of the technique called spacecraft tracking, but here realized with infrared laser light instead of radio waves. The laser light going out from the center spacecraft to the other corners is not directly reflected back because very little light intensity would be left over that way. Instead, in complete analogy with an RF transponder scheme, the laser on the distant spacecraft is phase-locked to the incoming light providing a return beam with full intensity again. After being transponded back from the far spacecraft to the center spacecraft, the light is superposed with the on-board laser light serving as a local oscillator in a heterodyne detection. This gives information on the length of one arm modulo the laser frequency. The other arm is treated the same way, giving information on the length of the other arm modulo the same laser frequency. The difference between these two signals will thus give the difference between the two arm lengths (i.e. the gravitational wave signal). The sum will give information on laser frequency fluctuations.

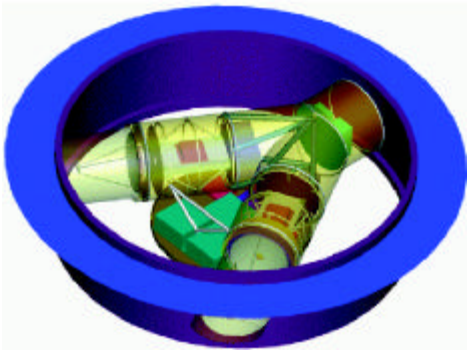

Figure 2: LISA Optical Assemblies

Each spacecraft contains two optical assemblies. The two assemblies on one spacecraft are each pointing towards an identical assembly on each of the other two spacecraft to form a Michelson interferometer. A 1W infrared laser beam is transmitted to the corresponding remote spacecraft via a 30-cm aperture f/1 Cassegrain telescope. The same telescope is used to focus the very weak beam (a few pW) coming from the distant spacecraft and to direct the light to a sensitive photodetector where it is superimposed with a fraction of the original local light. At the heart of each assembly is a vacuum enclosure containing a free-flying polished platinum-gold cube, 4 cm in size, referred to as the proof mass, which serves as an optical reference (``mirror'') for the light beams. A passing gravitational wave will change the length of the optical path between the proof masses of one arm of the interferometer relative to the other arm. The distance fluctuations are measured to sub-Ångstrom precision which, when combined with the large separation between the spacecraft, allows LISA to detect gravitational-wave strains down to a level of order $\Delta l / l = 10^{-23}$ in one year of observation, with a signal-to-noise ratio of 5.

The spacecraft mainly serve to shield the proof masses from the adverse effects due to the solar radiation pressure, and the spacecraft position does not directly enter into the measurement. It is nevertheless necessary to keep all spacecraft moderately accurately (10^{-8} m/√Hz in the measurement band) centered on their respective proof masses to reduce spurious local noise forces. This is achieved by a "drag-free" control system, consisting of an accelerometer (or inertial sensor) and a system of electrical thrusters.

Capacitive sensing in three dimensions is used to measure the displacements of the proof masses relative to the spacecraft. These position signals are used in a feedback loop to command micro-Newton ion-emitting proportional thrusters to enable the spacecraft to follow its proof masses precisely. The thrusters are also used to control the attitude of the spacecraft relative to the incoming optical wavefronts, using signals derived from quadrant photodiodes. As the three-spacecraft constellation orbits the Sun in the course of one year, the observed gravitational waves are Doppler-shifted by the orbital motion. For periodic waves with sufficient signal-to-noise ratio, this allows the direction of the source to be determined to arc minute or degree precision, depending on source strength.

Each of the three LISA spacecraft has a launch mass of about 400 kg (plus margin) including the payload, ion drive, all propellants and the spacecraft adapter. The ion drives are used for the transfer from the Earth orbit to the final position in interplanetary orbit. All three spacecraft can be launched by a single Delta II 7925H. Each spacecraft carries a 30 cm steerable antenna used for transmitting the science and engineering data, stored on board for two days, at a rate of 7 kbps in the X-band to the 34-m network of the DSN. Nominal mission lifetime is two years, but consumables are sized for an extended mission of more than 10 years.

LISA is envisaged as a NASA/ESA collaborative project, with NASA providing the launch vehicle, mission and science operations and about 50% of the payload, ESA providing the three spacecraft including the ion drives, and European institutes, funded nationally, providing the other 50% of the payload. The collaborative NASA/ESA LISA mission is aimed at a launch in the 2010 time frame. LISA is a Cornerstone mission in ESA's Future Science Program Horizons 2000 and has recently been included in NASA's Roadmap.

2 Technology Challenges

The LISA science objectives lead to the measurement requirements, which are to determine the changes of distance between test masses separated by $5x10^6$ km with picometer precision over a frequency range of 10^{-4} Hz to 10^{-1} Hz. The technology challenges are thus the development of a system to measure changes in distances between test masses, and of isolating the test masses from external disturbances so that changes in their separation due to gravitational waves are not masked by motions due to other forces. The technology developments needed are divided into the three areas of inertial sensors, micronewton thrusters, and picometer interferometry.

Each LISA spacecraft will carry two inertial sensors. The inertial sensors consist of a freely falling test mass, an enclosing housing with capacitor plates for sensing and forcing, a discharging subsystem, a caging mechanism, a venting mechanism and associated electronics. The inertial sensor will serve three interrelated functions. The design of the inertial sensor will limit unwanted disturbances from stray forces on the test mass to an acceptable level (i.e., less than that caused by gravitational waves between 0.0001 and 0.003 Hz). And, the inertial sensor will provide attitude and displacement information to the spacecraft for drag-free control.

As the defining end mirror of an interferometer arm, each test mass of an inertial sensor must have an acceleration noise less than $3x10^{-15}$ $m/s^2/Hz$ in the range of 0.0001 Hz to 0.003 Hz. For purposes of drag-free control, the inertial sensor must sense the position of the test mass with respect to its housing with a resolution of 10^{-9} m/Hz and the orientation with a resolution of $5x10^{-8}$ radian/Hz.

The LISA inertial sensor development is constrained by the fact that the desired performance cannot be demonstrated on the ground. Similar devices have been developed and tested on the ground at the level of 10^{-9} $m/s^2/Hz$, which is the practical limit to which the acceleration of 10 m/s^2 from the Earth's gravity can be removed by keeping one axis of the sensor orthogonal to the local gravity vector. Some space testing of inertial sensors has been done, and several missions are planned, with launches in the 2000-2002 time frame, that will employ sensors analogous to the LISA inertial sensors. These include Gravity-Probe B, whose gyroscope assembly will be also used as an inertial sensor for drag-free spacecraft control, and the CHAMP and GRACE missions which will employ accelerometers developed by ONERA to measure the atmospheric drag force.

From experience developed from building these devices, and from specific tests done to measure each possible noise source, it is possible to design an inertial sensor that will meet the LISA requirements. The types of noise forces that can affect the inertial sensor test mass can be identified and separately characterized in laboratory tests. Based on the noise models and tests, detailed instrument designs for inertial sensors meeting the LISA requirements have been completed. However this sensor cannot be operated, much less tested, in the Earth's gravity, making this a high-risk technology.

It is thus highly desirable to perform a flight demonstration of candidate inertial sensors. Such a test would consist of two inertial sensors, each with a test mass with its own housing and electronics, on a single spacecraft. The performance would be validated by

using one for spacecraft drag-free control, and measuring the position of the second with respect to the first to show that both are following the same trajectory, under the influence of gravitational forces only. Any non-gravitational force would appear as a change in the position of one test mass with respect to the other.

Some of the noise forces on the test mass are caused by fluctuations in the distance between the test mass and the rest of the spacecraft. For example, the spacecraft mass has a gravitational pull on the test mass and thus fluctuations in the position of the spacecraft cause fluctuations in the force on the test mass. Because of this the position of the spacecraft must be controlled to stay centered on the test mass. The position control requirements, derived from the inertial sensor requirements, in turn place requirements on the spacecraft thrusters. With the current mission design, the thrusters are required to have a thrust noise of about 10^{-7} N, with a continuous thrust of about 25 μN in order to oppose the force from solar radiation pressure. A new class of micronewton thrusters is needed to meet these requirements.

The best candidates for meeting these requirements are small ion thrusters which have been developed, partly under funding by ESA, for satellite station keeping and for satellite charge control. These devices operate by ionizing and accelerating atoms from a liquid-metal reservoir. These Field-Emission Electric Propulsion (FEEP) thrusters provide thrust in the desired range, with very high efficiency, allowing a very small amount of propellant to last for more than the 3 year LISA prime science mission.

The thrust, and the thrust noise, of these thrusters has so far not been directly measured. Instead the thrust characteristics have been derived by measurements of the ion current and applied voltage to compute the applied thrust. There are possibly errors in this computation if there are ejecta other than single ionized atoms (i.e. droplets). The thrust is difficult to measure directly because it is so small. However work is underway in Europe to develop torsion balance experiments to directly measure the thrust.

3 Developments in LISA Proof Mass Position Sensors

It has been repeatedly stated that[21], at low frequency, the performance of LISA as a gravitational wave detector is limited by the purity of geodesic motion of the test-masses that form the end mirrors of the three interferometer arms. By purity of geodesic motion, we mean here the absence of forces of non gravitational origin and of gravitational forces generated by sources on board the spacecraft. These have to be kept below $3\times10^{-15}\ \mathrm{N}/\sqrt{\mathrm{Hz}}$ at 0.1 mHz.

In each LISA spacecraft, a "drag-free" control loop, driven by a test-mass displacement sensor, tries to null, for both test-masses located on board the spacecraft, the relative displacement between the spacecraft and the test-mass along the axis ô identified by the laser beam impinging on it.

In this condition, the disturbance force f_o acting on each test-mass along ô, is divided, to a first approximation, in two categories[22]. To the first of these categories belong the stray forces $f_{s,o}$, that do not depend on the position of the test-mass relative to the spacecraft, e.g. thermal noise, displacement sensor back-action etc. The second category includes

the forces that originate from the linear, spring-like coupling of the test-mass $k_{oi}x_{S/C,I}$, to the residual motion $x_{S/C,I}$, of its i^{th} degree of freedom with respect to the spacecraft. In summary:

$$f_o = f_{s,o} + \sum_i k_{oi} x_{S/C,i}$$

Several sources of disturbance determine the overall budget for $x_{S/C,i}$: noisy forces acting on the spacecraft, cross-talking of control along different degrees of freedom and the noise of the relative displacement sensor. Minimizing the sources that are related to the displacement sensor itself often causes the coupling expressed by the coefficients k_{oi} to increase more rapidly than $x_{S/C,i}$ decreases. An optimized design of LISA inertial masses and sensor thus demands a modeling of all different sources of stiffness and noise and a multi-parameter optimization process.

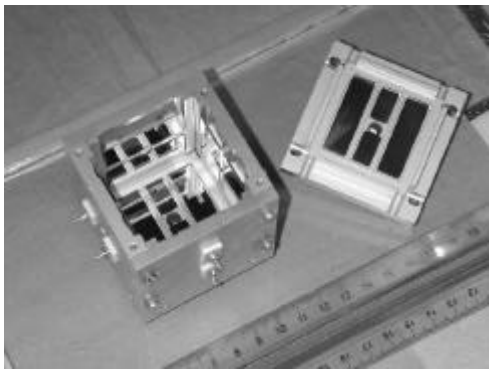

Figure 3: A laboratory prototype of the sensor. The part on the right is the top cover of the assembly that has been removed to show the electrodes. The small electrodes on the top cover are used to bias the test/mass. The test-mass is also not shown.

The device we are developing is based on a cubic test-mass surrounded by a set of electrodes that sense the motion along its 6 degrees of freedom. Test-mass motion modulates the capacitance of the electrodes relative to the test-mass itself by changing the gaps between the electrodes and the test-mass. This design gives equal sensitivity to the displacement along two axes and gives also equal sensitivity to rotation around two axes. The sensing electrode area, and thus sensitivity, for the two remaining degrees of freedom is slightly reduced in order to provide space for "injection" electrodes needed toAC bias the sensor. Figure 3 illustrates the electrode configuration in our laboratory prototype.

Though the design can be implemented with different materials, we are presently investigating a high thermal conductivity metal-ceramic technology. The enhanced thermal distortion obtained with the metal housing, relative to a high stability glass, is outweighed in our design by the superior suppression of thermal gradients[22]. One can show indeed[23] that thermal distortion of the housing, with typical thermal expansion coefficients in the range of $\alpha \approx 10^{-5}\ K^{-1}$, only becomes relevant if temperature fluctuations exceed $1\,K/\sqrt{Hz}$, a thermal instability many orders of magnitude worse than the figures allowed for LISA[21].

Readout electronics are based on a standard resonant bridge scheme (Figure 4) where the capacitance modulation of two opposing electrodes due to the test-mass motion x is detected as an imbalance of the bridge.

Capacitors C_{p1} and C_{p2}, nominally equal, are chosen to resonate with the differential transformer, maximizing the signal-noise ratio for a given drive frequency ω_o and transformer primary inductance, $L_1 \approx L_2$. Motion of the test mass imbalances the sensing capacitances C_{x1} and C_{x2}, producing a signal out of phase with the driving voltage.

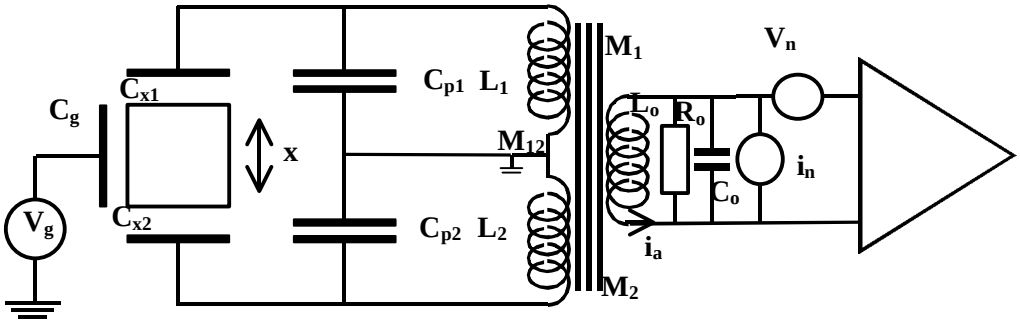

Figure 4: reference circuit for the evaluation of inertial sensor performance. To 0^{th} order the bridge is assumed to be symmetric so that $L_1=L_2=L$, etc. The transformer output inductance is $L_o=n^2L$. The generator marked i_n represent both the amplifier current noise and the thermal noise due to loss in the transformer.

We have assembled a breadboard version of the sensor readout shown in Figure 4. The 100 kHz AC bias source is a crystal oscillator with a feedback controlled amplitude based on the design in Ref 24.

In Figure 6 we present a measurement of the PSD of bridge output noise in the presence and in absence of bridge bias. Noise in excess of our predictions is found for frequencies below $\approx 10^{-2}$ Hz. However this excess is in agreement, in order of magnitude, with the noise calculated from thermal distortion of the low quality test bench used for the test.

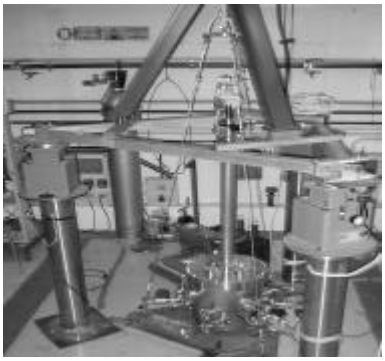

Figure 5: The torsion pendulum based test bench for the sensor. The picture shows (a) the vibration-isolation pods. (b)The torsion suspension of the apparatus. (c) The high vacuum chamber. (d) The micro-positioning system to center the electrode housing relative to the test-mass

Figure 7 shows preliminary results for the oscillation of the test-mass once suspended to a copper torsion fiber. The experiment has been performed in air and the torsion mode at 25 mHz is highly damped as expected. As the experiment has been performed on a laboratory desk and not within the isolated bench of Figure 5, noise is dominated by vibration noise. Also evident is the pendulum mode of the test-mass. This is due to the use of only one pair of facing electrodes, a geometry that couples equally well to torsion and to displacement.

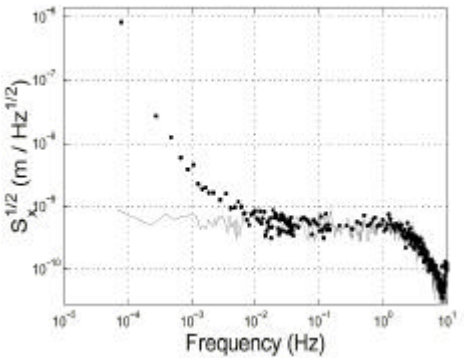

Figure 7: Displacement Noise PSD
Line: No Bias. Dots: With Bridge Bias

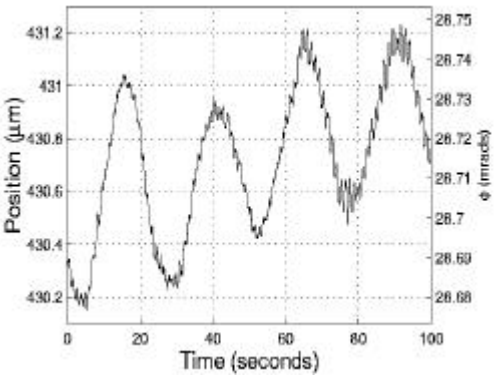

Figure 8: Oscillations of the Test Mass
Suspended on a Copper Fiber

The preliminary tests presented here only probe the displacement. The test on the torsion pendulum bench planned for the very near future will also test for stiffness and stray forces. A sensitivity goal of around 5×10^{-13} N/√Hz at ≈ 1 mHz is foreseen and would put a very interesting upper limit to many of the listed disturbances.

4 Detection of Coalescing Black Holes by LISA

The characteristic frequency to which LISA is sensitive is comparable to the orbital frequency at the innermost stable orbit of Schwarzschild black holes of mass $M_{BH} \sim 10^6\ M_{sun}$. With high sensitivity to periodic sources, one of the more promising "guaranteed" sources for LISA is the gravitational radiation from the final stages of coalescence of low mass (1 – 1000 M_{sun}) compact objects with low mass massive black holes ($M_{BH} \sim 10^{6\pm1}\ M_{sun}$).

Previous papers[25-29] considered the likely rate for detectable signals from degenerate compact objects in the cusps of normal galaxies, coalescing with central black holes such as the one inferred to be present in the Milky Way. Estimates for detectable signal rates are of the order one per year from these sources, but the estimates are sensitive to systematic uncertainties in the population contributing to the signal, with very large (many orders of magnitude) cumulative formal uncertainties in the expected signal rate. Since high rates of coalescence are self--limiting (through depletion of low mass compact objects at high coalescence rates; or the growth of the primary through coalescences, to the point where the frequency of the innermost stable orbit is too low for LISA to be sensitive to further coalescences), the formal uncertainty in the detectable rate is skewed to lower rates of coalescence than the "canonical" estimates in the literature. The true rate of detectable coalescences is sensitive to the assumptions about the mass function of the primary black hole, the number density of stars in regions where the appropriate mass black holes are found, and the mass and number of compact remnants available for coalescence in a Hubble time in such regions.

Assuming that low mass massive black holes exist in sufficient numbers, then the compact remnant of the stellar population near the black hole may coalesce with the central black hole. In particular, white dwarfs, neutron stars and low mass

(m_{BH} ~ 1 - 1000 M_{sun}) black holes present in the inner parsec around the central black hole will coalesce with the central black hole through emission of gravitational radiation. The typical starting orbit will be highly eccentric, and some fraction of the low mass compact objects will be lost through scattering straight into the central black hole, but calculations[26,27] suggest an appreciable rate for coalescences detectable by LISA. The primary uncertainties here are in the number density of remnants in the centers of galaxies. Neutron stars coalescence with central black holes is unlikely to be a significant contributor to the LISA rate, as natal kicks efficiently remove neutron stars from the inner parsec of the galaxies of interest. Low mass black holes are, however, of major interest as sources for LISA.

It is plausible that low mass black holes form from main sequence stars, with the progenitor zero age masses being ~25-30 M_{sun}. Assuming a Salpeter initial mass function, roughly one star in ten thousand leaves a low mass black hole with masses, m_{bh}, from as low as 2 M_{sun} up to ~100 M_{sun}.[33-35] The amplitude of gravitational radiation scales linearly with m_{bh}. LISA does better detecting coalescence of more massive low mass black holes at larger distances, if the gain in volume is greater than the reduced prevalence of the more massive low mass black holes. It seems likely that the initial population of low mass black holes in galactic nuclei is rapidly depleted through coalescence[28], in which case LISA may mostly detect coalescences from the epoch of star formation at z~1. At higher redshifts, the redshifting of the gravitational radiation to lower frequencies may reduce LISA's ability to detect coalescences, even for m_{bh} > 100 M_{sun}, except for MBH < 10^6 M_{sun}.

There are then two “best bet” scenarios for LISA detection of low mass black hole coalescence with low mass massive black holes. If there was significant nuclear star formation at z~1, then LISA may see strong signals from the initial flurry of coalescence of the initial population of low mass black holes with the central black hole. Alternatively, if there is replenishment of low mass black holes in the nuclei of Milky Way like spirals, the rate of coalescences detectable by LISA will be correspondingly higher.

There are two ways the low mass black hole population in spiral nuclei may be replenished. Either by formation of massive stars *in situ*, or by the transfer of low mass black holes from outside the inner nucleus. Recent observations suggests that the Milky Way has in fact formed massive stars in its nucleus in the recent past. Cotera et al[30] find several O or Wolf--Rayet stars in the inner parsec of the galaxy, some of which may be massive enough to form black holes. Certainly the Pistol Star[31] in the inner 100 pc of the Milky Way must collapse to a black hole. The number of high mass stars suggests an approximate rate of black hole replenishment of ~10^{-6} low mass black holes per year, with the mean rate of coalescence with the central black hole then necessarily ~10^{-6} y^{-1}. This implies a LISA event rate of 1 day^{-1}! More likely the current nuclear star formation rate is higher than the mean, but even if the duty cycle of such enhanced star formation is only 1%, the LISA event rate is enhanced proportionately. Alternatively, a cluster of stars formed outside the inner parsec of a spiral nucleus, may, if compact enough, be brought to the center by dynamical friction[32]. The recently reported observations of possible intermediate mass black holes[33-35], suggest the prospects for LISA observations are even better than previous estimates, if the mass estimates for these objects turn out to be accurate.

5 Detection of Cataclysmic Variables by LISA

General Relativity predicts that binary systems of stars produce gravitational waves (GWs) of significant intensity. Here we are particularly interested in the cataclysmic variable binaries (CVs). These systems emit low frequency GWs, $<10^{-3}$ Hz, therefore capable of being detected by LISA.

A CV is a semi-detached binary system of low mass and very short orbital period. The primary star is an accreting degenerate white dwarf and the secondary one is usually, but not always, a late-type star that fills its critical Roche lobe and transfers mass to the companion. There are 1020 CVs classified[38] and more than 300 of them have known periods[39].

Due to the fact that positive detections of CVs by LISA might be improved once we know the sources beforehand, we compile in the present study a catalogue of CVs, for which we know at least their orbital periods and distances. We present here a catalog with 156 CVs where 37 of them have GW amplitudes greater than the S/N = 1 LISA curve and also appear above the binary confusion noise curve, therefore, capable of being detected at this signal-to-noise ratio.

We argue that the present study is of interest since in the literature one has not found a systematic identification of possible detectable GW CVs, since an early study made by Douglass & Braginsky[37] twenty years ago, and also a preliminary study by Aguiar et al[36].

We argue that it would be of interest whether other groups performed a similar study for the other binary systems which produce low frequency GWs in the frequency band where LISA is sensitive.

It is worth mentioning that a positive detection of a binary system through its gravitational emission, with some help of electromagnetic data observations, could lead one to know all the parameters related to the binary system, namely, the masses of the stars, their distances to the earth, the period of the system and their orientation angles.

6 Cosmology with LISA

Primordial GW stochastic backgrounds provide us a picture of the state of the Universe, and the corresponding behavior of fundamental fields, at very-early cosmic times and high energies. Theoretical predictions of the spectrum Ω_{gw} of the primordial background are extremely difficult as they involve physics beyond the standard model of which we have little understanding if any; here we take as reference value, in order to benchmark the performance of an instrument, the prediction from standard slow-roll inflationary scenarios: $\Omega_{gw} \sim 10^{-16} - 10^{-15}$ for 10^{-16} Hz f 1 GHz [42,43].

The optimal strategy to detect a stochastic background involves the cross-correlation of the data streams from two instruments with uncorrelated noise[41]. Ungarelli and Vecchio[44] have recently discussed the sensitivity that can be achieved by cross-correlating the outputs of two identical LISA's, separated by a distance D on the same orbit. Depending on the distance and relative orientation of the detectors, one can reach

$5\times10^{-14} \le h_{100}^2 \Omega_{gw}^{(\min)} \le 10^{-12}$, for a for a false alarm probability of 5%, and a detection rate of 95%; however, one cannot fully exploit this remarkable instrumental sensitivity in searching for primordial signals. In fact, most of the signal-to-noise ratio (SNR) is accumulated in the band around 1 mHz; here the astrophysically generated background $\Omega_{gw,g}(f)$ is strong[40]; in searches for a primordial background $\Omega_{gw,p}(f)$, the optimal filter unavoidably picks up a spurious residual contribution due to $\Omega_{gw,g}(f)$, that cannot be removed. The radiation from unresolved binary systems provides therefore a *fundamental sensitivity limit* in searching for the primordial GW background; this limit, in the case of an experiment carried out with a pair of twin LISA's, is $h_{100}^2 \Omega_{gw,p}^{(\min)} \ge 5\times10^{-13}(e/0.1)$; ε is the fraction of the astrophysically generated background that is still present in the data because it can not be removed by using statistical properties such as the degree of anisotropy.

The mHz frequency window is therefore unsuitable to reach a sensitivity able to test slow roll inflation. One needs to design an experiment with optimal sensitivity in a band free from generated backgrounds. The most promising region seems to be ~0.1 Hz – 1 Hz -- accessible by LISA-like interferometers with arms shorter by a factor ~100 - due to the presence backgrounds from ~10^{-7} Hz to ~0.1 Hz generated by massive black hole binary systems, white dwarf binaries and neutron stars binaries; for f0.1 Hz the number of sources per frequency bin becomes less than one, and one can in principle identify and remove each spectral line, cleaning the band. How this can be effectively done and what is the SNR that is required to achieve this cleaning is an open question that needs to be addressed carefully. Clearly the technological challenge is considerable; the main noise sources that would degrade the performance of such a detector are the shot noise, beam pointing fluctuations and accuracy of the phase measurement technique. This imposes stringent requirements on the power and frequency of the laser, as well as on the dimensions of the "optics" and on other aspects of the instrument.

References

1. Lyne, A.G. and D.R. Lorimer, Nature. 1994. p. 127.
2. Tutukov, A.V. and L.R. Yungelson, MNRAS. 1993. p. 675.
3. Misner, C.W. et al. Gravitation. Freeman & Co., San Francisco, 1973.
4. Saulson, P.R. "Fundamentals of Interferometric Gravitational Wave Detectors." World Scientific, Singapore, 1994.
5. Schutz, B.F. A First Course in General Relativity. Cambridge University Press, Cambridge, 1985.
6. Thorne, K.S. *Gravitational Radiation*, in: S.W. Hawking and W. Israel, eds., 300 Years of Gravitation. Cambridge University Press, Cambridge, 1987. pp. 330--458.
7. Weber, J. Phys. Rev. 1960. p.306.
8. Bassan, M. Class. Quant. Grav. Supplement A. 1994. p.11.
9. Pirani, F.A.E. Acta Physica Polonica. 1956. p. 389.
10. Gertsenshtein, M.E. and V.I. Pustovoit, JETP. 1963. p. 433.
11. Weiss, R. Quarterly Progress Report of RLE, MIT. 1971. p. 54.
12. Moss, G.E., L.R. Miller, and R.L. Forward, Appl. Opt. 1971. p. 2495.
13. Abramovici, A., et al. Science. 1992. p. 325.
14. Bradaschia, G. et al., Nucl. Instrum. and Methods A. 1990. p. 518.

15. Danzmann, K et al. "GEO600 – A 300 m Laser-interferometric Gravitational Wave Antenna", Proc. Edoardo Amaldi Conference, Frascati, June 1994; and also: J. Hough et al, Proc. MG7, Stanford, July 1994.
16. unpublished, see: http://133.40.8.83/TAMA.HTM. 1996.
17. unpublished, see: http://tamago.mtk.nao.ac.jp. 1996.
18. Tsubono, K. and TAMA collaboration, "TAMA Project" in: K. Tsubono, M.-K. Fujimoto, K. Kuroda, eds. Gravitational Wave Detection, Proc. TAMA Intern. Workshop. Nov. 1996, Universal Academy Press (Tokyo), 1997. p. 183-191.
19. Tsubono, K. and TAMA collaboration, " TAMA Project" in: K. Tsubono, M.-K. Fujimoto, K. Kuroda, eds. Gravitational Wave Detection, Proc. TAMA Intern. Workshop, Nov. 1996, Universal Academy Press (Tokyo), 1997. p. 183-191.
20. Kaspi, V.M., J.H. Taylor, and M.F. Ryba, Astrophys. J. 1994. p. 713.
21. Bender, P., et al., LISA Pre-Phase A Report, Max Planck Institude for Quantum Optics, MPQ233-1998.
22. Vitale, S. and R. Dolesi. "Gravitational Waves." Proc. of the 3rd Edoardo Amaldi Conference, Pasadena 1999, AIP Conf. Proc. 523, p. 231 (1999).
23. "Drag Free Satellite Control." ESTEC Contract #13691/99/NL/FM (SC), Technical Proposal.
24. Hueller, M. Laurea Thesis, University of Trento (2000).
25. Sigurdsson, S., in Proc. 2nd International LISA Symposium, AIP Conf. Proc. 456, p. 53 (AIP New York)
26. Hils, D., Bender, P.L., ApJL, 445, 1995. pp. L7-10.
27. Sigurdsson, S., Rees, M.J., MNRAS, 284, 1997. pp. 318-326.
28. Sigurdsson, S., Classical and Quantum Gravity, 14, 1997. pp. 1425-1429
29. Miralda-Escude, J., Gould, A., ApJ, submitted (2000) (astro-ph/0003269)
30. Cotera, A.S., Figer, D.F., Blum, R.D., in ``Wolf-Rayet stars in the framework of stellar evolution." ed. J.M. Vreux, A. Detal, D. Fraipont-Caro, E. Gosset, and G. Rauw,1996. Liege: Universite de Liege, p.429.
31. Figer, D.F., et al., ApJ, 506, 1998. pp. 384-404.
32. Polnarev, A.G., Rees, M.J., A & A, 283, 1994. pp. 301-312.
33. Ptak, A., Griffiths, R., ApJL, 517, 1999. pp. L85--L89.
34. Matsumoto, H., et al, ApJL, in press. 2000.
35. Kaaret, P., et al, MNRAS, in press. 2000.
36. Aguiar, O.D., de Araujo, J.C.N., Meliani, M.T., Jablonski, F.J., Ara\'ujo, M.E. AIP Conference Proceedings: Second International LISA Symposium on the Detection and Observation of Gravitational Waves in Space, ed. W.M. Folkner, Woodbury, New York, Vol. 456, 1998. p. 87
37. Douglass, D.H., Braginsky, V. B. General Relativity, an Einstein Centenary Survey. eds. S.W. Hawking, W. Israel, Cambridge University Press, Cambridge, 1979.
38. Downes, Webbink, Shara, 1997, PASP 109, p. 345.
39. Ritter, H. and Kolb, U., 1998, A&AS 129, p. 83.
40. Hils, D., Bender, P.L., and Webbink, R.L., *Astrophys. J.*, **360**, 75, 1990.
41. Flanagan, E., *Phys. Rev. D*, **48**, 2389, 1993.
42. Krauss, L., and White, M., *Phys. Rev. Lett.* **69**, 869, 1992.
43. Turner, M., *Phys. Rev. D*, **55**, 435, 1997.
44. Ungarelli, C., and Vecchio, A., submitted to *Phys. Rev D.*